NACA

RESEARCH MEMORANDUM

for the

Bureau of Ships, Department of Navy

PRELIMINARY INVESTIGATION OF A TECHNIQUE FOR

STABILITY STUDIES OF A SELF-PROPELLED

MODEL OF A SUBMERGED SUBMARINE

By Robert E. McKann and William W. Petynia

Langley Aeronautical Laboratory
Langley Field, Va.

NATIONAL ADVISORY COMMITTEE
FOR AERONAUTICS

WASHINGTON

APR 15 1954

NATIONAL ADVISORY COMMITTEE FOR AERONAUTICS

RESEARCH MEMORANDUM

for the

Bureau of Ships, Department of Navy

PRELIMINARY INVESTIGATION OF A TECHNIQUE FOR

STABILITY STUDIES OF A SELF-PROPELLED

MODEL OF A SUBMERGED SUBMARINE

By Robert E. McKann and William W. Petynia

SUMMARY

The initial development of a technique for the qualitative study of the stability and control characteristics of a free, self-propelled, dynamic submarine model was made in Langley tank no. 1.

An evaluation was made of two types of control systems. With a system that provided a constant rate of control deflection (similar to that used on full-scale submarines) the model could not be handled at the desired test speeds. A self-centering, flicker-type control with an automatic trimming device, designed for use in the Langley free-flight-tunnel models, permitted the model to be trimmed and controlled at speeds corresponding to 30 knots full scale.

Power and control were transmitted to the model through a trailing cable. The tests were confined to two-dimensional dive maneuvers. For most of the tests the trailing cable was located at the center of buoyancy, but some investigation was made with the trailing cable attached at the stern and with a self-propelled follower, either of which would permit a three-dimensional maneuver. The experimental paths were reproducible. Calculations of the model path and motions were made by using stability derivatives obtained from wind-tunnel tests made at the Reynolds number of the tank tests. Reasonable agreement was obtained between the experimental and calculated paths.

INTRODUCTION

The changes in speed and configuration currently being made in submarines have emphasized the need for methods to evaluate the stability and control of new designs. The available data and theory that can be used to predict these characteristics for new configurations are limited. The effects of minor changes can be obtained from tests of the full-size submarine, although, investigation of major changes by this method is generally impractical or prohibitive because of the expense or hazards involved.

The problems associated with the maneuvering of submarines while submerged are somewhat similar to those encountered with aircraft. It is expected, therefore, that wind-tunnel techniques, which have been successful in studying the flight characteristics of aircraft and in evaluating the effect of design parameters, might be applied directly.

In the case of complex stability and control problems of aircraft, a useful tool has been a simplified free-flight dynamic model controlled by an operator through a trailing cable. Although the scale of such models is small, it has been established that they provide adequate qualitative information for many purposes and permit reliable predictions of full-size characteristics when careful attention is given to scale effects.

In order to make application of the basic philosophy and accumulated experience of NACA free-flight-model techniques to studies of the submarine, the Bureau of Ships, Department of the Navy, requested that the initial development of a corresponding method for use of a submerged body in a towing tank be undertaken by the Langley Laboratory. The development was carried only to a point where its feasibility could be demonstrated, at which time the model and associated equipment were transferred to the staff of the David Taylor Model Basin for refinement and application to submarine investigations outside the scope of NACA's activities.

PRELIMINARY CONSIDERATIONS

Typical procedures for evaluating the stability and control characteristics of aircraft in the Langley free-flight tunnel are described in reference 1. Briefly, the models are flown in the tunnel in a steady glide or under their own power when required, and various maneuvers are executed by a trained remote operator. The principal data are the observations of the "pilot" and motion-picture records of the model behavior. Measurements of the model motions and path are sometimes made,

as well as measurements of the forces acting under steady conditions to permit the use of pertinent theory in predicting full-scale flying qualities more closely.

In application of the free-flight technique to the submarine model, retention of the simplicity of the technique was taken as the basic requirement. For this reason, the size of the model was chosen as the smallest compatible with mechanical design, and the trailing cable was retained to supply power for propulsion and controls. The limitations of the tank boundaries were also necessarily considered in choosing the scale.

Again the principal data would be the observations of the pilot, which obviously become of greatest value after experience with a variety of configurations and types of control. Measurements of the motions and path of the model and, in addition, measurements of force data would permit a comparison between the experimental and theoretical paths and motions.

The most important maneuver to be investigated was assumed to be the dive and pull-out within the limits of the pressure depth and water surface. The critical nature of this maneuver was assumed to require measurement of the actual path in space and some correlation of the paths with those calculated by theory.

As in the case of the airplane, the free model becomes of greatest assistance in investigating complex maneuvers involving other than the vertical plane. Some consideration was therefore given to arrangements of the trailing cable that would impose minimum restraint in three-dimensional maneuvers such as a climbing or diving turn.

SYMBOLS

The orientation of the body axes having the center of buoyancy of the model as the origin is shown in figure 1. The arrows indicate the positive direction of moments, deflections, and forces, which, with the exception of the positive sense of the Z axis, are as given in reference 2.

d maximum diameter of model, ft

q dynamic pressure, $\frac{1}{2}\rho V^2$, lb/sq ft

V speed along flight path, fps

ρ mass density of water, slugs/cu ft

k_2 coefficient of transverse added water mass

m   mass of model, slugs

$$C_{L_c} = \frac{\partial\left(F_c/qd^2\right)}{\partial(\sin\beta)}$$

$$C_{L_\alpha} = \frac{\partial\left(F_\alpha/qd^2\right)}{\partial\alpha}$$

$$C_{L_\delta} = \frac{\partial\left(F_\delta/qd^2\right)}{\partial\delta}$$

$$C_{L_{\dot\theta}} = \frac{\partial\left(F_{\dot\theta}/qd^2\right)}{\partial(\dot\theta d/2V)}$$

$$C_{m_\alpha} = \frac{\partial\left(M_\alpha/qd^3\right)}{\partial\alpha}$$

$$C_{m_{mg}} = \frac{\partial\left(M_{mg}/qd^3\right)}{\partial(\sin\theta)}$$

$$C_{m_c} = \frac{\partial\left(M_c/qd^3\right)}{\partial\left[\sin(25.6-\beta)\right]}$$

$$C_{m_\delta} = \frac{\partial\left(M_\delta/qd^3\right)}{\partial\delta}$$

$$C_{m_{\dot\theta}} = \frac{\partial\left(M_{\dot\theta}/qd^3\right)}{\partial(\dot\theta d/2V)}$$

D_c trailing-cable tension, lb

F_c lift force due to trailing cable, $D_c \sin\beta$, lb

F_α lift force due to angle of attack of model, lb

F_δ lift force due to elevator deflection, lb

$F_{\dot\theta}$ lift force due to angular velocity of model, lb

$I_{c.b.}$ moment of inertia of model about transverse body axis through center of buoyancy, slug-ft^2

M_c moment about center of buoyancy due to cable drag, ft-lb

M_{mg} moment about center of buoyancy due to model weight, ft-lb

M_α moment about center of buoyancy due to angle of attack of model, ft-lb

M_δ moment about center of buoyancy due to elevator deflection, ft-lb

$M_{\dot\theta}$ moment about center of buoyancy due to pitching velocity of model, ft-lb

X longitudinal body axis

Y lateral body axis

Z vertical body axis perpendicular to XY

X_O fixed longitudinal axis located in plane of undisturbed water surface directed forward

Y_O fixed lateral axis located in plane of undisturbed water surface directed to starboard

Z_O fixed vertical axis directed upward

α angle of attack of model measured between longitudinal body axis and model path, deg

β angle between longitudinal body axis and trailing cable at point of attachment, positive in the sense of rotation from the X_O to the Z axis, deg

γ model path angle measured between path and water surface, deg

$\dot\gamma$ rate of change of model path angle, deg/sec

δ elevator deflection, measured from center line of model, deg

θ pitch angle, measured between the center line of model and water surface, deg

$\dot\theta$ angular velocity, radians/sec

$\ddot\theta$ angular acceleration, radians/sec^2
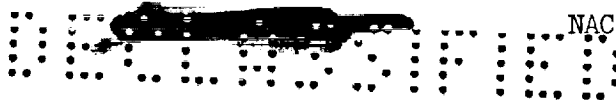
DESCRIPTION OF MODEL

The model, designated Langley tank model 281, was a 2.62 percent model of the Bureau of Ships submarine design SST Scheme III without superstructure or conning tower. A photograph of the model is shown in figure 2.

Exterior Form

Hull.- The hull was a body of revolution and had an overall length of 5.0 feet with a length-diameter ratio of 7.0 and a gross weight of 75 pounds (volume, 1.19 cu ft). The equation for the body of revolution is given in reference 3 as

$$u^2 = \sum_{n=1}^{n=6} a_n v^n$$

and $r_1 = \dfrac{R_1 L}{d^2}$; also $r_o = \dfrac{R_o L}{d^2}$.

where

u	nondimensional diameter, $\dfrac{U}{d}$
v	nondimensional station aft of nose, $\dfrac{V}{L}$
U	maximum diameter at station V, ft
V	station aft of nose, ft
r_o	nondimensional nose radius
r_1	nondimensional tail radius
R_o	nose radius, ft
R_1	tail radius, ft
L	overall length of model, ft
d	maximum diameter of model, ft

and

$$a_1 = +1.0000$$

$$a_2 = +1.1372$$

$$a_3 = -10.7749$$

$$a_4 = +19.7843$$

$$a_5 = -16.7925$$

$$a_6 = +5.6460$$

$$r_0 = 0.50$$

$$r_1 = 0$$

The center of buoyancy and center of gravity were located 2.3 feet from nose and were, respectively, on the body axis and 0.055 foot below the body axis.

Tail surfaces.- Cruciform tail surfaces were located on the stern just ahead of the propeller. The elevators and stabilizers had an area of 12.5 and 6.5 square inches, respectively. The rudders had an area of 11.5 square inches with 6.9 square inches of fin area. The tail surfaces and their plan form are shown in figure 3.

Propeller.- Thrust was provided by a propeller located at the stern on the body axis. The three-blade propeller had a diameter of 2.63 inches and a 7.87-inch pitch. A shroud ring attached at the blade tips reduced the possibility of damage to the trailing cable.

Interior Arrangement and Components

Hull.- A cutaway drawing showing the interior arrangement and structure of the model is presented in figure 3. The hull was divided into three sections. The forward and middle sections were of 1/16-inch spun aluminum, reinforced with bulkheads. These sections contained the ballast weights and cameras, respectively. The rear section was machined of 17S-T aluminum alloy to form a rigid mounting for the drive motor, autosyn unit, and control mechanisms.

The forward and middle sections were joined by a vacuum seal to permit easy access to the cameras and ballast. The rear section was attached to the middle section by a flanged joint and secured by screws about the circumference of the hull.

Ballast.- The ballast, located in the forward section of the hull, consisted of a cylindrical weight, on the center line, for adjustment of the fore-and-aft balance. An additional weight was located at the keel for adjustment of the lateral balance. To apply a static rolling moment to compensate for the propeller torque, the forward section was rotated in relation to the other sections prior to joining.

Cameras.- Two 16-mm gunsight motion-picture cameras (fig. 4) were located in the model center section facing port and starboard, perpendicular to a vertical plane through the body axis. The port camera was located at the center of buoyancy and the starboard camera at the same vertical location but 0.313 foot farther aft. Power to operate the cameras was supplied through the trailing cable.

Power installation.- A 0.5-horsepower d-c electric motor (fig. 5) with reduction gear was used to drive the propeller. Power was supplied to the drive motor through the trailing cable. The speed of the model was varied by means of a manually operated rheostat at the control station.

Control mechanisms.- High-speed electric motors were used to provide a control having a fixed deflection rate of the type in general use on submarines. Control movement was started by a switch which allowed the surfaces to be moved in either direction or stopped. Limit switches prevented over-travel. The control position at any instant was visible to the operator on a remote-reading autosyn located in the control station. A range of constant deflection rates from 15° to 90° per second (model size) was available. Overshoot at switch-off was reduced to a minimum by electrical braking.

A flicker control specifically designed for use in free-flight-tunnel models was also used. Although this control goes full-off and full-on, approximately proportional control may be obtained by regulating the frequency of control deflections and the length of time during which deflections are maintained. This control, shown in figure 6, employed an electrically actuated pneumatic mechanism which provided full deflection or return in approximately 0.1 second. The surface automatically returned to neutral position at switch-off. A self-trimming ratchet provided a mechanical shift of the neutral position which was proportional to the percentage of control motions made in a particular direction. The increment of shift of the neutral was adjustable.

In order to program accurately the elevators during a dive maneuver, a motor-driven cam mechanism was used to operate the control switches.

Air at 25 pounds per square inch was supplied to the pneumatic mechanism by a 1/8-inch-diameter, thin-walled plastic tube from a tank and regulator on the towing carriage. The exhaust from the control

mechanism was used in conjunction with a 7-pound-per-square-inch relief valve in the hull to pressurize the center and rear sections against water leakage. Air from the hull relief valve was exhausted at the tip of the top rudder.

APPARATUS AND PROCEDURE

Towing Carriage Setup

General arrangement.- The tests were conducted in a section $16\frac{1}{2}$ feet long located between the main carriage and auxiliary carriage of Langley tank no. 1 and bounded on the sides by grids 10 feet apart. (See fig. 7(a).) A description of Langley tank no. 1 and the towing carriage is given in reference 4.

Grids.- The grids (fig. 7(b)) consisted of standard 6-inch-mesh concrete reinforcing wire welded to streamlined steel tubes attached to the main and auxiliary towing carriages. The tops of the grids were positioned 6 inches below the water surface and extended to a depth of 10 feet. Numbered plastic flags in alternate squares were used to identify the location on the grid. The grids were photographed by the cameras within the model.

Control station.- The control station shown in figures 7 and 8 was located on the front of the main carriage 5 feet above the water surface looking down on the test section. The rheostat, switch, and ammeter for the main drive motor, the manual and program control switches, and the remote-reading control position autosyn were located at this station.

Trailing-Cable Arrangements

The trailing cable, comprising the necessary power and control leads, was approximately 1/4 inch in diameter and 60 feet in length. The cable consisted of twelve no. 35 seven-strand insulated copper wires and a 1/8-inch-diameter plastic tube. The plastic tubing was fastened to the wires to form a single lead to the model. To minimize the change in drag as the submergence of the model varied, the cable was attached to a streamlined strut at a point 5 feet below the water surface (fig. 7(b)).

Cable at center of buoyancy.- The cable (configuration (a) fig. 9) was divided and attached to the sides of the model on a transverse line just ahead of and above the center of buoyancy. The cable was rejoined by a bridle behind the model. This method of attaching the cable permitted the model to operate freely in pitch.

Cable at the stern.- Cable configuration (b) was attached to a rigid guide strip which carried the cable around the propeller as shown in figures 5 and 9. This point of cable attachment would permit a maneuver in three dimensions.

Self-propelled follower.- Cable configuration (c) shown in figure 9 was attached to the model as in the stern configuration and led to the nose of the self-propelled follower at a distance of 2 feet behind the submarine. The follower shown in figure 10 was constructed of aluminum and powered by a 1.3-horsepower variable-frequency electric motor. The thrust could be governed by a hydraulic propeller-pitch control mechanism actuated by the tension in the cable from the submarine to the follower. When a fixed propeller blade angle was set, the thrust could also be varied by operation of a rheostat at the control station. The propeller was located at the center of buoyancy of the follower and three large fins provided sufficient lift at small angles to the flow to maneuver the follower and the trailing cable with a minimum effect upon the motions of the submarine model.

Test Procedure

Prior to making the dive maneuver selected for these tests, the model was ballasted so that the dynamic trim and roll were zero, and the excess buoyancy was approximately 0.3 percent of the model weight.

With the thrust adjusted to the desired speed, the operator, by visual observation from the control station, trimmed the model to straight and level path approximately 2 feet below the water surface. References 5 and 6 indicate that the effects of surface proximity become small at depths greater than three body diameters. Once the model was trimmed the controls were switched from manual to automatic program control and the cameras were started. After completion of the dive the operator again resumed manual control of the model.

The same procedure was employed when the self-propelled follower was used. The path of the follower was governed by the submarine so that the submarine was relieved of most of the forces due to the trailing cable. Difficulties with the hydraulic system prevented the use of the follower for programmed dives.

The paths of the model were obtained from the motion pictures of the grids. The data obtained included the depth, angle of pitch, and distance from the leading edge of the grids. To obtain the horizontal displacement along the tank, the distance of the model from the leading edge of the grids was subtracted from the total distance the grid had moved along the tank. The path angle is the slope of the curve of depth against horizontal displacement. A detailed description of the data

DECLASSIFIED

reduction from the motion-picture film is included in the appendix. The maneuvers for which data are presented were made at a speed of 5 feet per second corresponding to 18 knots, full size.

Precision

The accuracy of the basic measurements is believed to be within the following limits:

```
Speed, fps . . . . . . . . . . . . . . . . . . . . . . . . . . . . . . . . . ±0.2
Angle of pitch, deg . . . . . . . . . . . . . . . . . . . . . . . . . . . ±0.5
Angle of yaw, deg . . . . . . . . . . . . . . . . . . . . . . . . . . . . ±0.5
Angle of roll, deg . . . . . . . . . . . . . . . . . . . . . . . . . . . ±0.5
Horizontal displacement, ft . . . . . . . . . . . . . . . . . . . . ±0.05
Lateral displacement, ft . . . . . . . . . . . . . . . . . . . . . . ±0.1
Vertical displacement, ft . . . . . . . . . . . . . . . . . . . . . ±0.05
```

EXPERIMENTAL RESULTS

Qualitative Analysis of Control Systems

The principal basis for evaluating the two control systems was the relative difficulty experienced by the operator in keeping the model on a straight and level submerged course. Control with the constant-rate-type system was difficult and became increasingly so as speed was increased, until, at a speed of 4 feet per second (15 knots full size), the operators could not hold the model on course. For this reason the model could not be trimmed out to allow the performance of dive maneuvers. The need for self-centering and trimming devices was readily apparent. With the self-centering and trimming flicker-type control system, the model could be trimmed to straight and level flight to the accuracy obtainable by visual observation from the control station. The model was then definitely controllable at the maximum model speed of 8 feet per second corresponding to 30 knots full size.

Dive Paths

Cable at center of buoyancy.- Data from two typical test runs in dive maneuvers with the cable attached near the center of buoyancy are presented in figure 11 as plots of pitch angle, path angle, vertical displacement, and elevator deflection against horizontal displacement along the tank.

A comparison of runs 1 and 2 indicates the ability to reproduce a maneuver. Although the model was not perfectly trimmed out before the maneuvers were begun (see the plot of pitch in fig. 11(b) during the first 6 feet of the run), generally good agreement between the maneuvers may be noted. The effect upon the motions of the model of displacement of the cable from the center of buoyancy to the position shown in figure 9(a) can be shown by calculation to be small. Additional refinement in the technique such as more accurate positioning and trimming of the model prior to the maneuver should result in more exact reproduction of the test maneuver.

Cable at stern.- Similar data for a dive maneuver (run 3) with the cable attached to the stern are presented in figure 12. The effect of the shift of point of cable attachment to the stern may be seen in figure 13. Stern attachment is seen to reduce the depth of dive to nearly one-half and the maximum angular displacements to about three-quarters of the values reached with the cable at the center of buoyancy. Although the general nature of the maneuver is similar, corrections would probably have to be made for the effect of the trailing cable in order to obtain accurate data with this configuration.

ANALYSIS

Equations of Motion

The path of the model during a dive maneuver with the cable at the center of buoyancy was calculated by an iterative procedure suggested by Mr. Charles H. Zimmerman, Stability Research Division of the Langley laboratory using the lift and moment equations for the body in submerged flow and the sign convention of figure 1. The summation of the lift forces referred to path axes is:

$$mV\dot{\gamma} = F_\alpha + F_\delta + F_{\dot{\theta}} + F_c \tag{1}$$

and the moments about the center of buoyancy are:

$$I_{c.b.}(1 + k_2)\ddot{\theta} = M_\alpha + M_\delta + M_{\dot{\theta}} + M_c + M_{mg} \tag{2}$$

Expressed in coefficient form for time, t, equations (1) and (2) become[1]:

$$mV\dot{\gamma}_t = qd^2\left(C_{L_\alpha}\alpha_t + C_{L_\delta}\delta_t + C_{L_{\dot{\theta}}}\frac{\dot{\theta}_t d}{2V} - C_{L_c}\sin\beta_t\right) \tag{3}$$

---

[1]The effect of the force resulting from the acceleration perpendicular to the path was found by calculation to be small for the type of maneuver investigated and is therefore neglected.

$$I_{c.b.}(1 + k_2)\ddot{\theta}_t = qd^3\left[C_{m_\alpha}\alpha_t + C_{m_\delta}\delta_t + C_{m_{\dot\theta}}\frac{\dot\theta_t d}{2V} - C_{m_{mg}}\sin\theta_t + \right.$$

$$\left. C_{m_c}\sin(25.6 - \beta_t)\right] \tag{4}$$

The angles, angular velocity, and depth at each successive time, t, were determined from the following relations:

$$\dot\theta_t = \dot\theta_{t-1} + \ddot\theta_{t-1}\,\Delta t \tag{5}$$

$$\theta_t = \theta_{t-1} + \left(\frac{\dot\theta_{t-1} + \dot\theta_t}{2}\right)\Delta t \tag{6}$$

$$\gamma_t = \gamma_{t-1} + \dot\gamma_{t-1}\,\Delta t \tag{7}$$

$$\alpha_t = \theta_t - \gamma_t \tag{8}$$

$$z_t = z_{t-1} + v\left(\frac{\sin\gamma_{t-1} + \sin\gamma_t}{2}\right)\Delta t \tag{9}$$

The required stability derivatives were obtained in the Langley free-flight tunnel on the rotary and six-component balances at a Reynolds number corresponding to that of the tank tests. The drag of the trailing cable was determined from static thrust calibrations. The lift and moment applied to the model by the cable were determined from the cable angle and the location of the cable attachment. The location of the cable attachment is shown in figure 14. This position allowed the cable to be photographed by the port camera during the maneuver and permitted the angle of the trailing cable relative to the model to be measured. A typical plot of the cable angle relative to the model center line for two maneuvers is shown in figure 15.

Comparison with Experimental Paths

The calculated values of pitch, path angle, and vertical displacement of the model with the cable at the center of buoyancy against horizontal distance for runs 1 and 2 are compared with the experimental values

in figures 16 and 17. The experimental initial conditions of trim, trimming velocity, trimming acceleration, path angle and depth, as well as the elevator sequence used in the run, were assumed for the calculations. No account was taken in the calculations for the effect of surface proximity or the variation in cable force due to the change in cable path during the maneuver. While good agreement was obtained between the calculated values and experimental maneuvers, it is probable that better agreement would result from correction for these factors.

No calculations were made for the stern configuration since the angle of the trailing cable for these maneuvers was not known.

CONCLUDING REMARKS

The preliminary investigation for stability studies of model submarines has shown that a self-centering and trimming flicker-type mechanism for operating the model control surfaces permits the model to be trimmed and controlled at speeds corresponding to 30 knots full size.

The experimental maneuvers were approximately reproducible. Reasonable agreement was also obtained between the calculated and experimental results, although more exact cable data are necessary for precise duplication. Attachment of the cable at the stern, as might be required for a three-dimensional maneuver, imposed considerably more restraint on the model than attachment at the center of buoyancy. The self-propelled follower, however, offers a promising means for reducing the cable restraint.

The use of the self-propelled small model with a trailing cable appears to provide a rapid means for obtaining the general stability and control characteristics. Internal cameras photographing a towed grid provide accurate path data. The model paths may be compared with calculated values when Reynolds number and trailing-cable effects are taken into account.

Langley Aeronautical Laboratory,
    National Advisory Committee for Aeronautics,
        Langley Field, Va., April 6, 1954.

Robert E. McKann
Aeronautical Research Scientist

William W. Petynia
Aeronautical Research Scientist

Approved:
    John B. Parkinson
Chief of Hydrodynamics Division

cg

APPENDIX

DATA REDUCTION

The following procedure was used to compute the position of the model from motion pictures of the towed grids which formed the sides of the test section. A camera speed of eight frames per second gave a sufficient number of data points to record the time history of the motions of the model up to the maximum test speed. The elevator position and camera frames were recorded against time.

The data obtained from the film were x_p and x_s'', the horizontal distance from the grid leading edge to the intersection of the camera line of sight with the port and starboard grids, respectively; z_p and z_s'', the vertical distance from the water surface to the same intersections; d_p and d_s, the lengths of the grid recorded by the port and starboard cameras, respectively; and θ', the pitch angle projected into the vertical longitudinal plane as read from the data film.

These data were determined for each frame and plotted against time. Faired values were then used and the position of the model was calculated for 0.2-second intervals, which corresponded to intervals of about 1 foot along the tank, since the maneuvers for which data were obtained were made at a forward speed of 5 feet per second.

In order to define the motions and the paths of the model from the above data, expressions for the location of the model are derived for a camera position at the center of buoyancy. Corrections to these expressions for the rearward displacement of one of the cameras are then determined. The orientation of the body axes of the model relative to the fixed axes is shown in figure 1. The intersection of the line of sight of the cameras on the screen for cameras at the center of buoyancy and with the starboard camera displaced rearward are shown in figure 18.

Symbols

The following symbols apply only to this appendix.

a   projection of camera displacement distance on X_0 axis, ft

b   longitudinal camera displacement from center of buoyancy, ft

d_p, d_s length of grid recorded by port and starboard cameras, respectively, as determined from the grid scale, ft

NACA RM SL54D21

k   lateral distance between grids, ft

t   time, sec

Δt time interval between successive calculations, sec

x,y,z   distances measured parallel to corresponding fixed axes, ft

X,Y,Z   body axes

X_0,Y_0,Z_0 fixed axes

θ pitch angle measured between model center line and horizontal
             plane, deg

θ' projection of pitch angle on grid (angle read from camera
             data), deg

ψ yaw angle measured between model center line and plane of
             grid, deg

ϕ roll angle measured between horizontal plane and transverse
             body axis Y of model, deg

ϕ' projection of roll angle on fixed transverse plane Y_0Z_0
             (angle read from camera data), deg

Subscripts and primes:

c.b.   center of buoyancy of model

p   port grid

s   starboard grid

'   projection of pitch or roll angle

"   condition for displacement of starboard camera off center of
             buoyancy of model

Derivation of Equations

On the assumption that both cameras are located at the center of
buoyancy, the proportionality of the length of the grid recorded by the
camera to the distance from the camera to the grid may be used to deter-
mine the lateral position of the model; that is,

$$\frac{y_s}{y_p} = \frac{d_s}{d_p} \tag{A1}$$

Since the distance between the grids is constant,

$$y_s + y_p = k \tag{A2}$$

Substituting y_p from equation (A2) into equation (A1) gives

$$y_s = \frac{kd_s}{d_p + d_s} \tag{A3}$$

or substituting y_s from equation (A2) into equation (A1) gives:

$$y_p = \frac{kd_p}{d_p + d_s} \tag{A4}$$

where y_p and y_s are horizontal distances from the center of buoyancy to the port and starboard grids, respectively. The values of d_p and d_s are determined from the data film and k, the lateral distance between grids, is known.

According to the relationships shown in figure 18,

$$\tan \psi = \frac{x_s - x_p}{k} \tag{A5}$$

$$x_{c.b.} = x_s - y_s \tan \psi \tag{A6}$$

and

$$x_{c.b.} = x_p + y_p \tan \psi \tag{A7}$$

Substituting from equations (A4) and (A5) into equation (A7) yields

$$x_{c.b.} = \frac{x_p d_s + x_s d_p}{d_p + d_s} \tag{A8}$$

where $x_{c.b.}$ is the horizontal distance from the center of buoyancy to the grid leading edge.

From figure 18,

$$\tan \phi' = \frac{z_s - z_p}{k} \tag{A9}$$

$$z_{c.b.} = z_s - y_s \tan \phi' \tag{A10}$$

Substituting from equations (A3) and (A9) into equation (A10) gives

$$z_{c.b.} = \frac{z_p d_s + z_s d_p}{d_p + d_s} \tag{A11}$$

where $z_{c.b.}$ is the vertical distance from the center of buoyancy to the water surface.

The foregoing expressions are for the conditions where both cameras are located at the center of buoyancy. If the starboard camera is displaced rearward a given distance b, the effect of this displacement on the measurements obtained from the film must be determined before the location of the model can be computed from the preceding relations.

The measurements obtained from the port camera are unchanged, but measurements from the starboard camera are now x_s'', z_s'', and d_s''. The relation between these new readings and x_s, z_s, and d_s with the starboard camera at the center of buoyancy must be determined. The angle θ' is measured directly, but angles ψ and ϕ' are considered separately.

The ratio of the distance along the line of sight and the length of grid recorded by the camera is constant. With the camera at the center of buoyancy the distance along the line of sight is $y_s(\sec^2\phi' + \tan^2\psi)^{1/2}$. Likewise, with the camera displaced aft, the distance along the line of sight is $(y_s + a \tan \psi)(\sec^2\phi' + \tan^2\psi)^{1/2}$. Similarly as in equation (A1)

$$\frac{y_s(\sec^2\phi' + \tan^2\psi)^{1/2}}{(y_s + a \tan \psi)(\sec^2\phi' + \tan^2\psi)^{1/2}} = \frac{d_s}{d_s''} \tag{A12}$$

Simplifying this equation results in

$$d_s = \frac{d_s{}'' y_s}{y_s + a \tan \psi} \tag{A13}$$

Substituting d_s from equation (A13) into equation (A3) gives

$$y_s = \frac{k d_s{}'' - a d_p \tan \psi}{d_p + d_s{}''} \tag{A14}$$

where y_s is the distance from the center of buoyancy to the starboard grid and a may be defined from figure 18 as:

$$a = \frac{b}{(\sec^2\theta' + \tan^2\psi)^{1/2}} \tag{A15}$$

From figure 18,

$$x_{c.b.} = x_s{}'' - y_s \tan \psi - a \sec^2\psi \tag{A16}$$

and

$$z_{c.b.} = z_s{}'' - (y_s + a \tan \psi)\tan \phi' - a \tan \theta' \tag{A17}$$

where $x_s{}''$ and $z_s{}''$ are determined directly from the film, y_s from equation (A14), and a is defined by equation (A15).

From figure 18,

$$\tan \psi = \frac{x_s{}'' - x_p - a \sec^2\psi}{k} \tag{A18}$$

Substituting for a from equation (A15) yields

$$\tan \psi = \frac{x_s{}'' - x_p}{k} - \frac{b}{k \cos^2\psi (\sec^2\theta' + \tan^2\psi)^{1/2}} \tag{A19}$$

Likewise, from figure 18,

$$\tan \phi' = \frac{1}{k}\left[z_s{}'' - y_s \tan \phi' - a \tan \psi \tan \phi' - a \tan \theta' - z_p + y_s \tan \phi'\right]$$

(A20)

Simplifying equation (A20) gives

$$\tan \phi' = \frac{z_s{}'' - a \tan \theta' - z_p}{k + a \tan \psi}$$

(A21)

Substituting for a from equation (A15) into equation (A21) results in

$$\tan \phi' = \frac{z_s{}'' - z_p}{k} - \frac{b(\tan \theta' + \tan \psi \tan \phi')}{k(\sec^2\theta' + \tan^2\psi)^{1/2}}$$

(A22)

The true pitch and roll angles are determined from the projected pitch and roll angles, as measured from the camera data by the following relations:

$$\tan \theta = \tan \theta' \cos \psi$$

(A23)

$$\tan \phi = \tan \phi' \cos \psi$$

(A24)

REFERENCES

1. Shortal, Joseph A., and Osterhout, Clayton J.: Preliminary Stability
   and Control Tests in the NACA Free-Flight Wind Tunnel and Correlation
   With Full-Scale Tests. NACA TN 810, 1941.

2. Anon.: Nomenclature for Treating the Motion of a Submerged Body
   Through a Fluid. Tech. and Res. Bull. No. 1-5, Soc. of Naval Arch.
   and Marine Eng., Apr. 1950.

3. Gertler, Morton: Resistance Experiments on a Systematic Series of
   Streamlined Bodies of Revolution - For Application to the Design
   of High-Speed Submarines. Rep. C-297, David Taylor Model Basin,
   Navy Dept., Apr. 1950.

4. Truscott, Starr: The Enlarged N.A.C.A. Tank, and Some of Its Work.
   NACA TM 918, 1939.

5. Pond, H. L.: The Moment Acting on a Spheroid Moving Under a Free
   Surface. Rep. C-489 (NS 715-084), David Taylor Model Basin,
   Navy Dept., Mar. 1952.

6. Brooks, S. H., Weinblum, G., and Young, D. B.: Forces and Moments
   Experienced by a Spheroid Moving Uniformly On or Near the Surface.
   Rep. C-384 (NS 715-084), David Taylor Model Basin, Navy Dept.,
   June 1951.
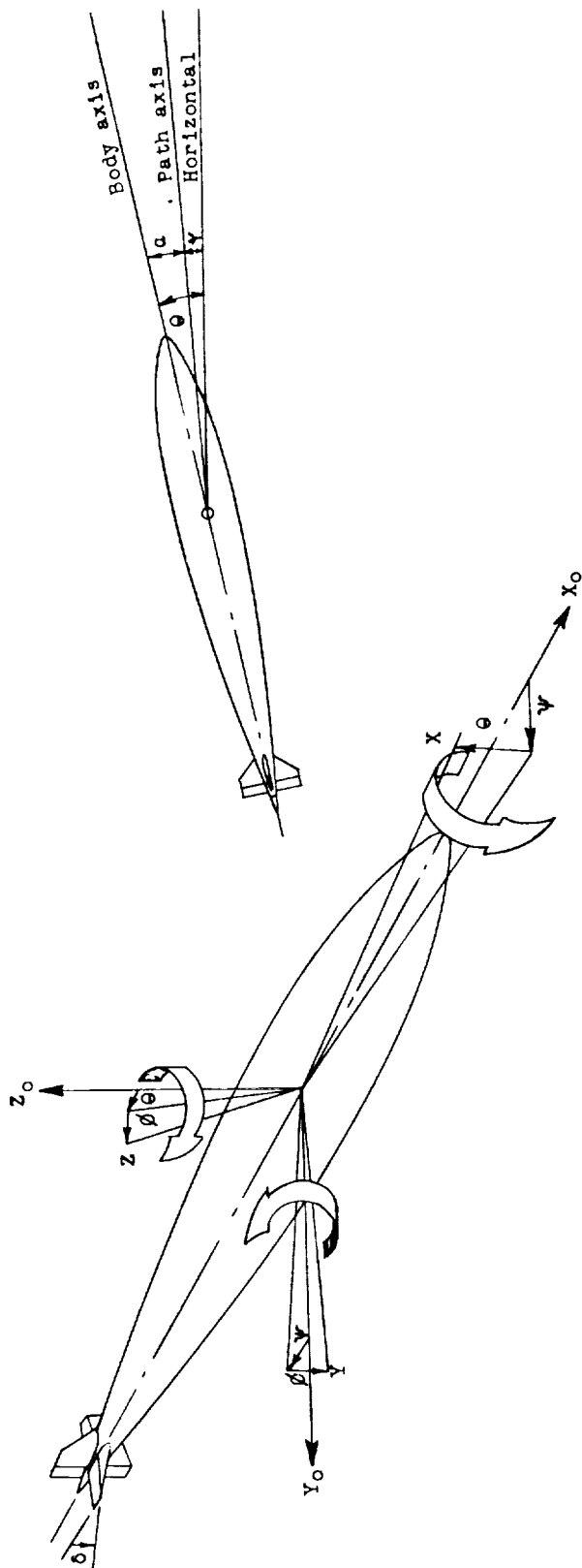
(Arrows indicate the positive direction of moments, deflections, and forces)

X, Y, Z	Body axes
X_o, Y_o, Z_o	Fixed axes
ψ	Angle of yaw, measured in X_oY_o plane, taken about Z_o axis
θ	Angle of pitch measured between longitudinal body axis and horizontal
ϕ	Angle of roll, measured in the YZ plane, taken about the X axis
α	Angle of attack, measured between longitudinal body axis and path
γ	Path angle, measured between path and horizontal

Figure 1.- Orientation of the body.

Figure 2.- Three-quarter front view of Langley tank model 281.

L-83654

Propeller shroud

Air exhaust tube

Rear section

Control mechanism

Drive motor

Middle section

Cameras

Vacuum seal

Adjustable weight

Forward section

8.5"

8.5"

Top

36"

24"

8.5"
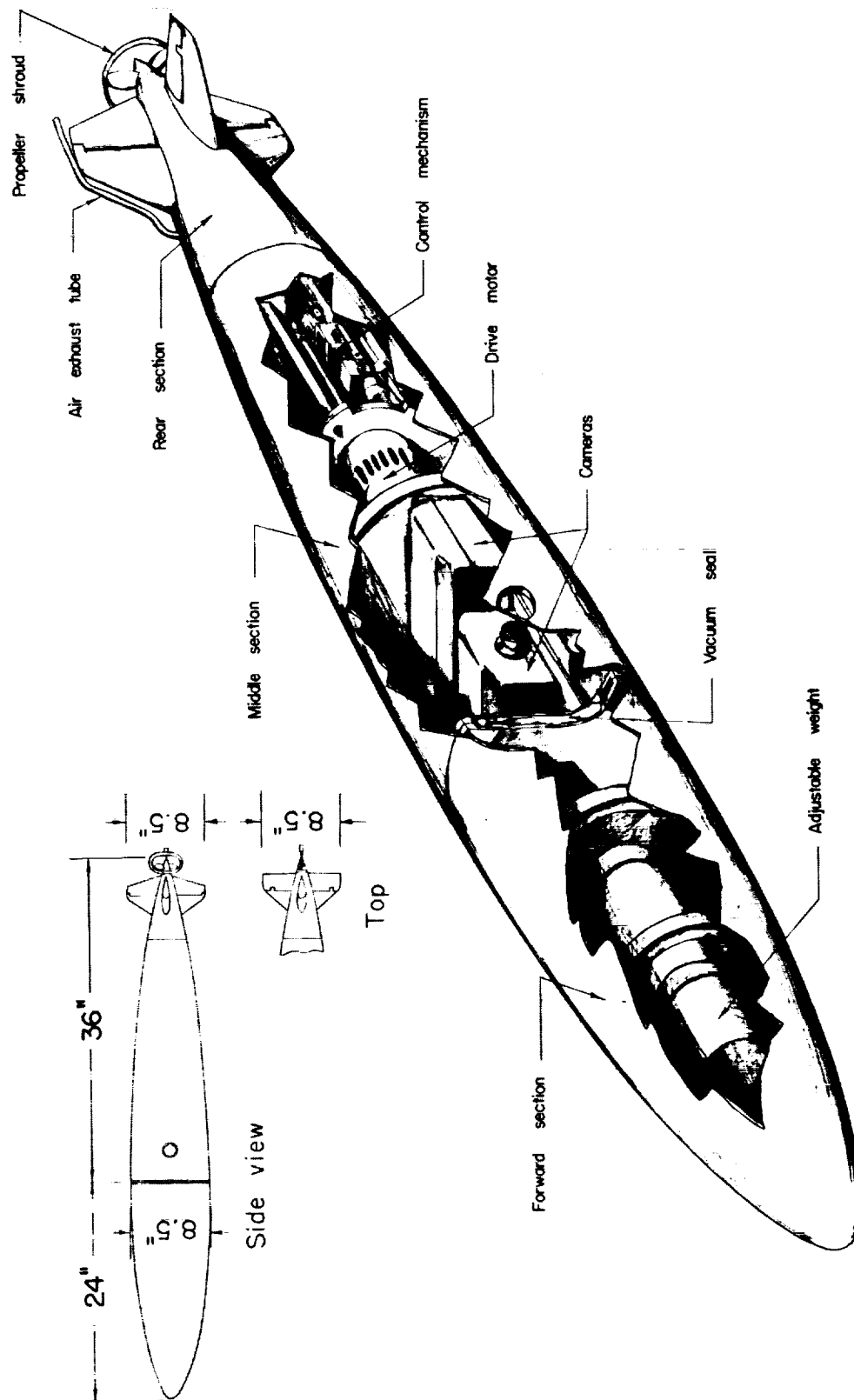
Side view

Figure 3.- Cutaway view of Langley tank model 281.
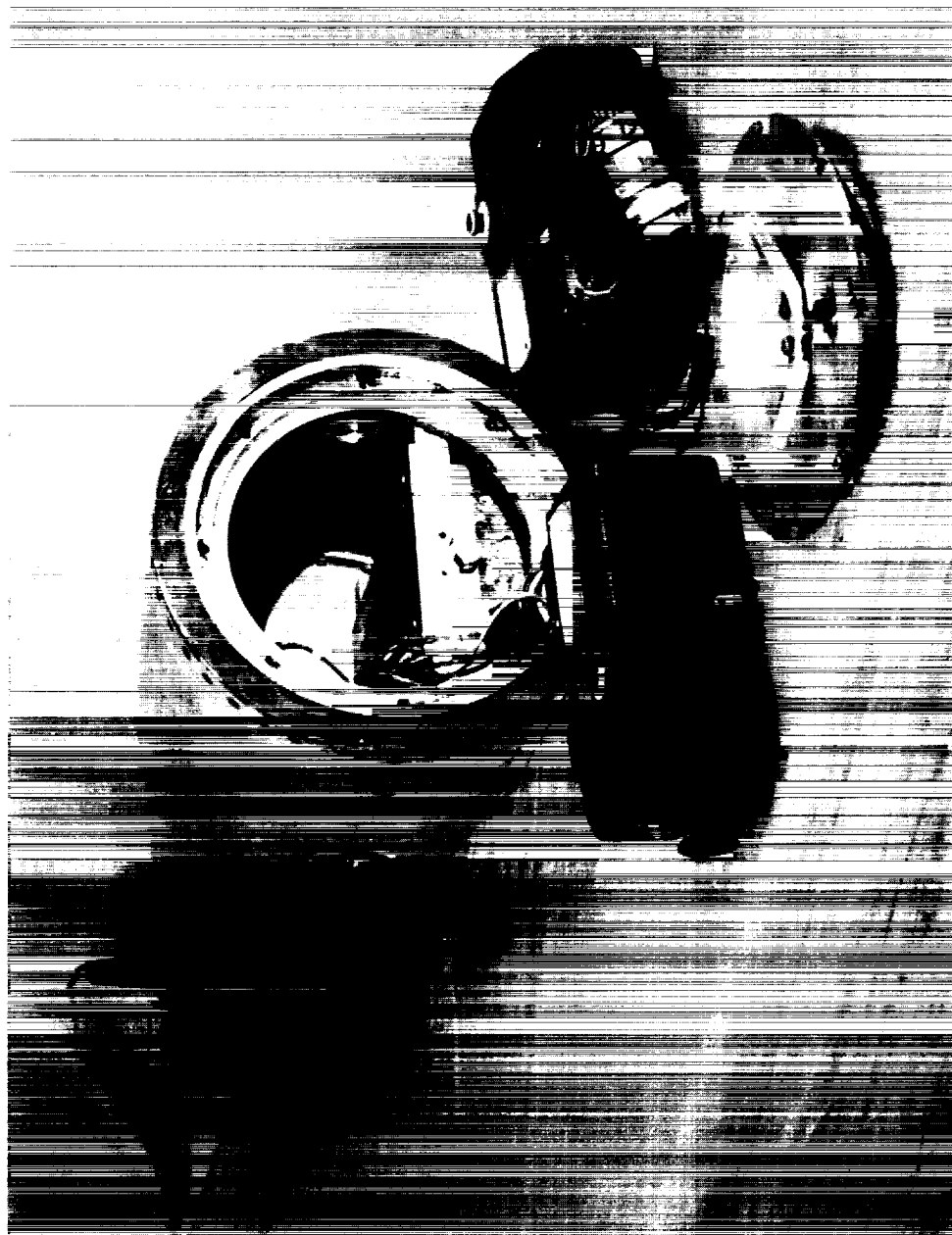
L-83655

Figure 4.- Front view of middle section of Langley tank model 281 with
cameras removed.
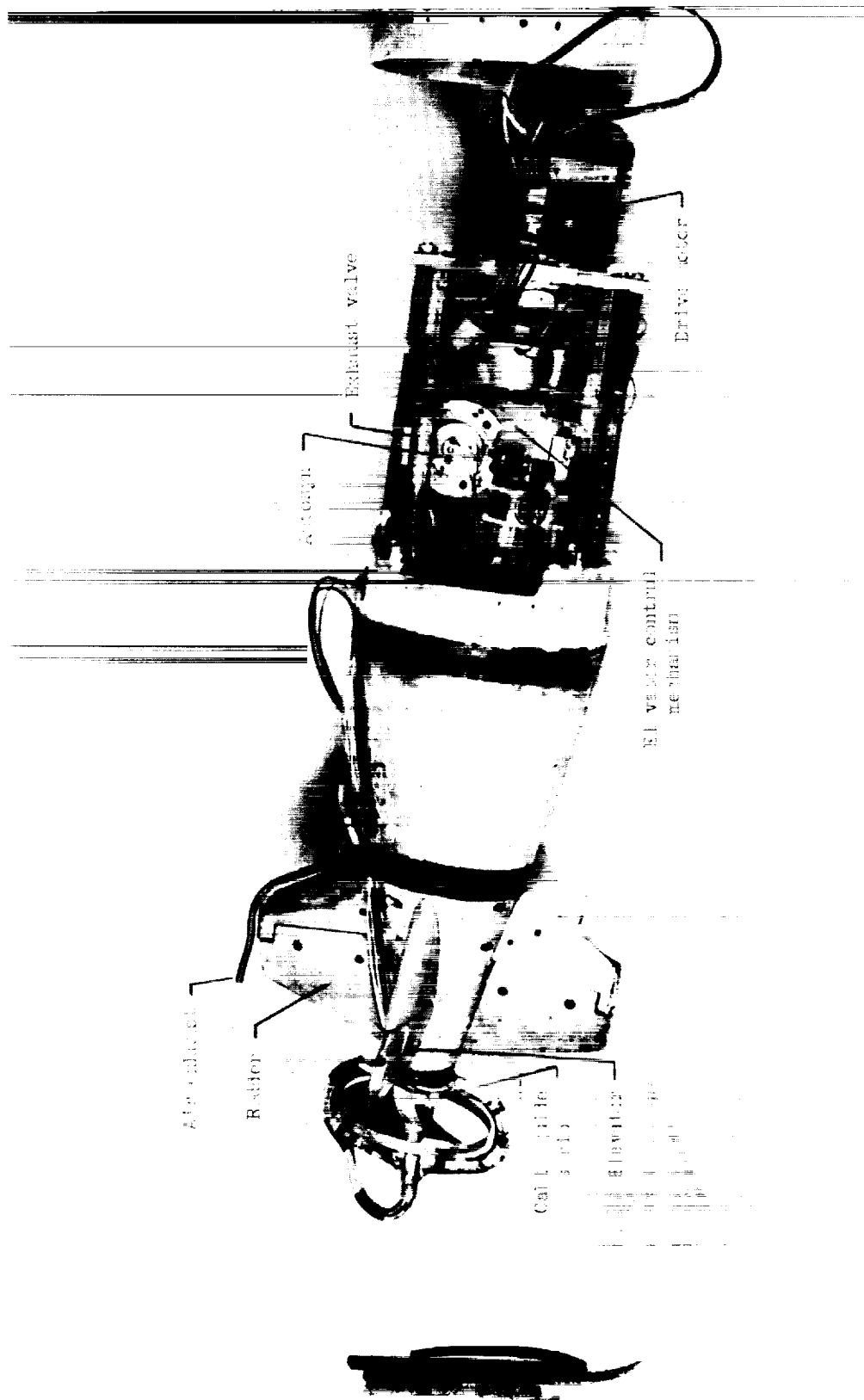
L-83656

Figure 5.- Side view of rear section of Langley tank model 281.
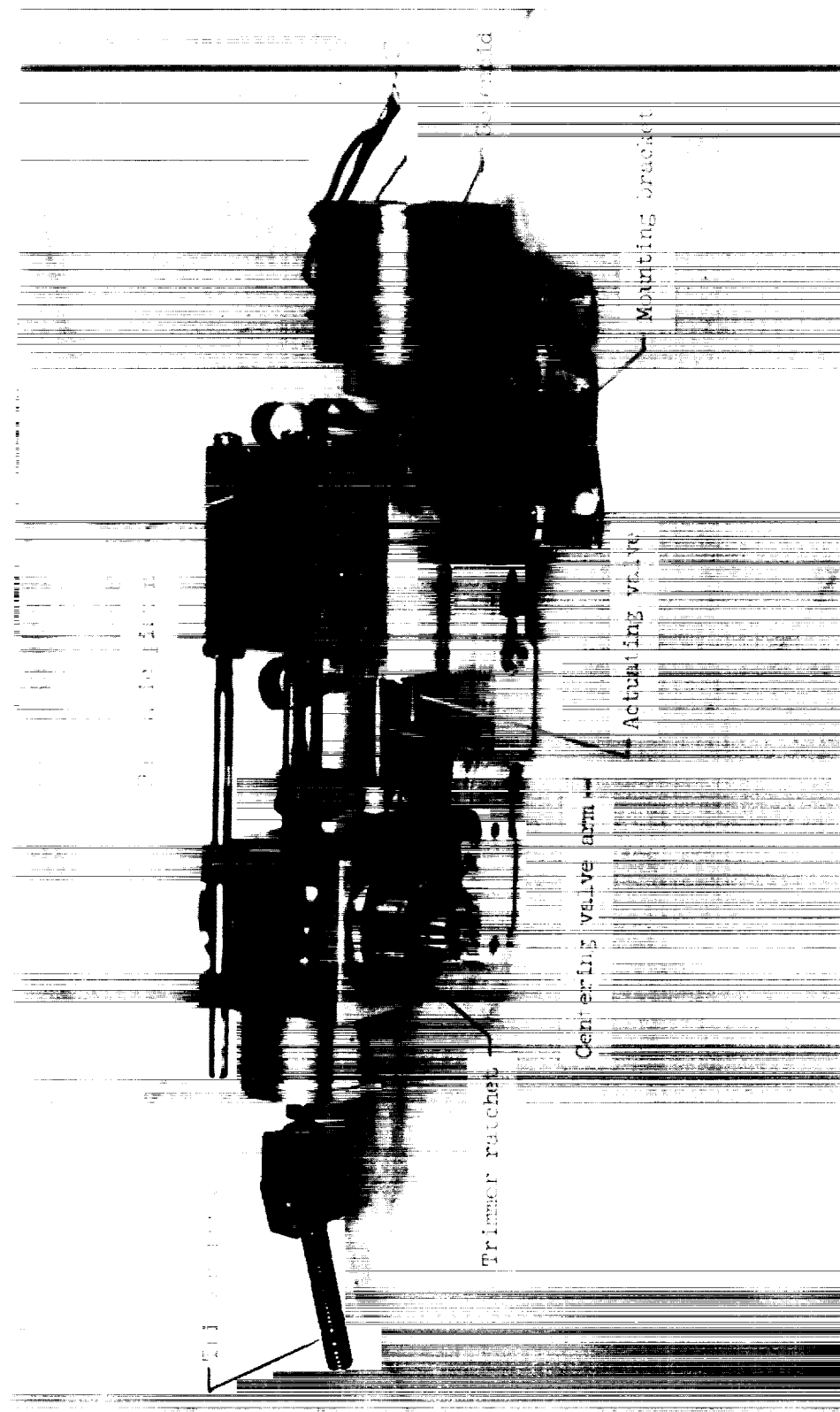
Figure 6.- Flicker-type control mechanism.
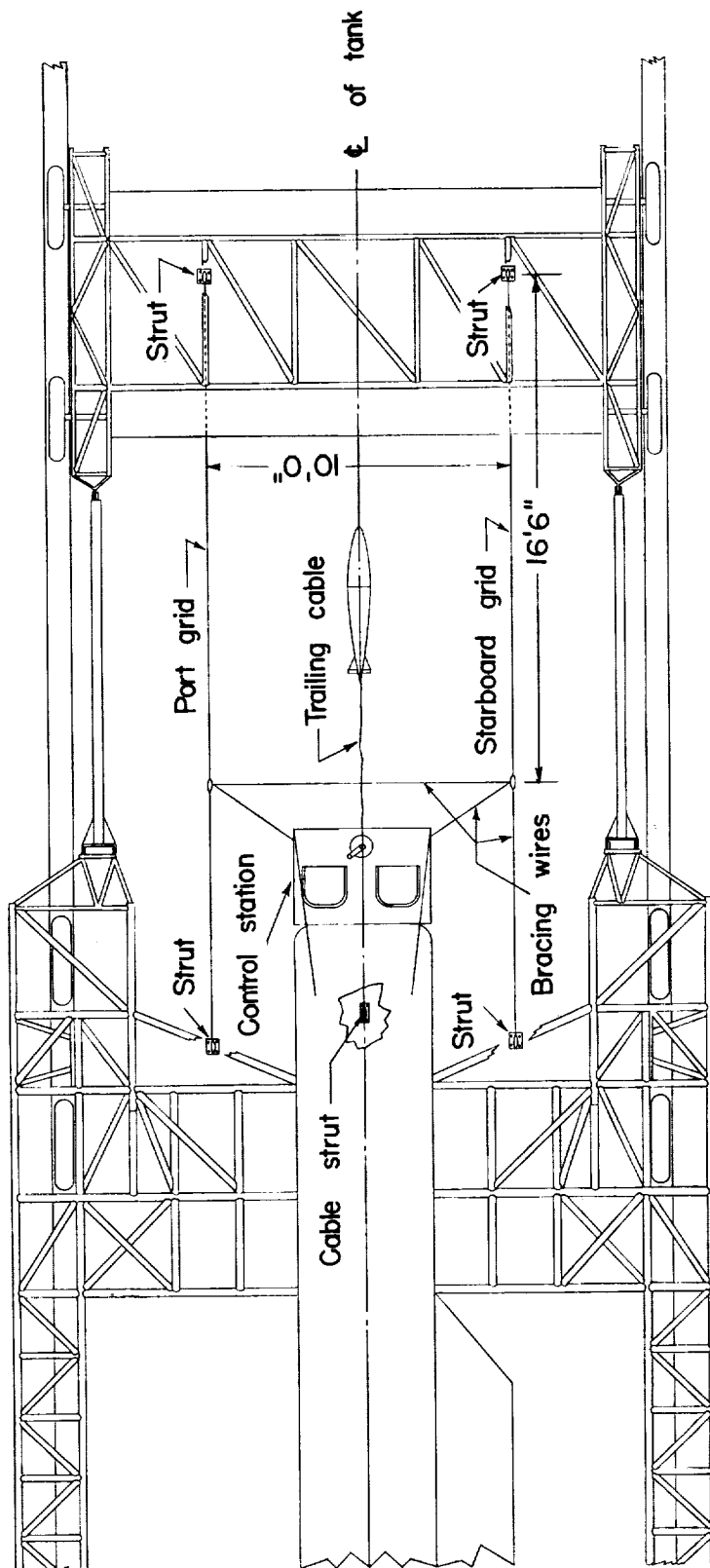
L-83657

Figure 7.- Views of towing carriage and test apparatus.

(a) Top view.

Strut

Strut

10'0"

Port grid

Trailing cable

Starboard grid

16'6"

Strut

Control station

Bracing wires

Strut

Cable strut

€ of tank
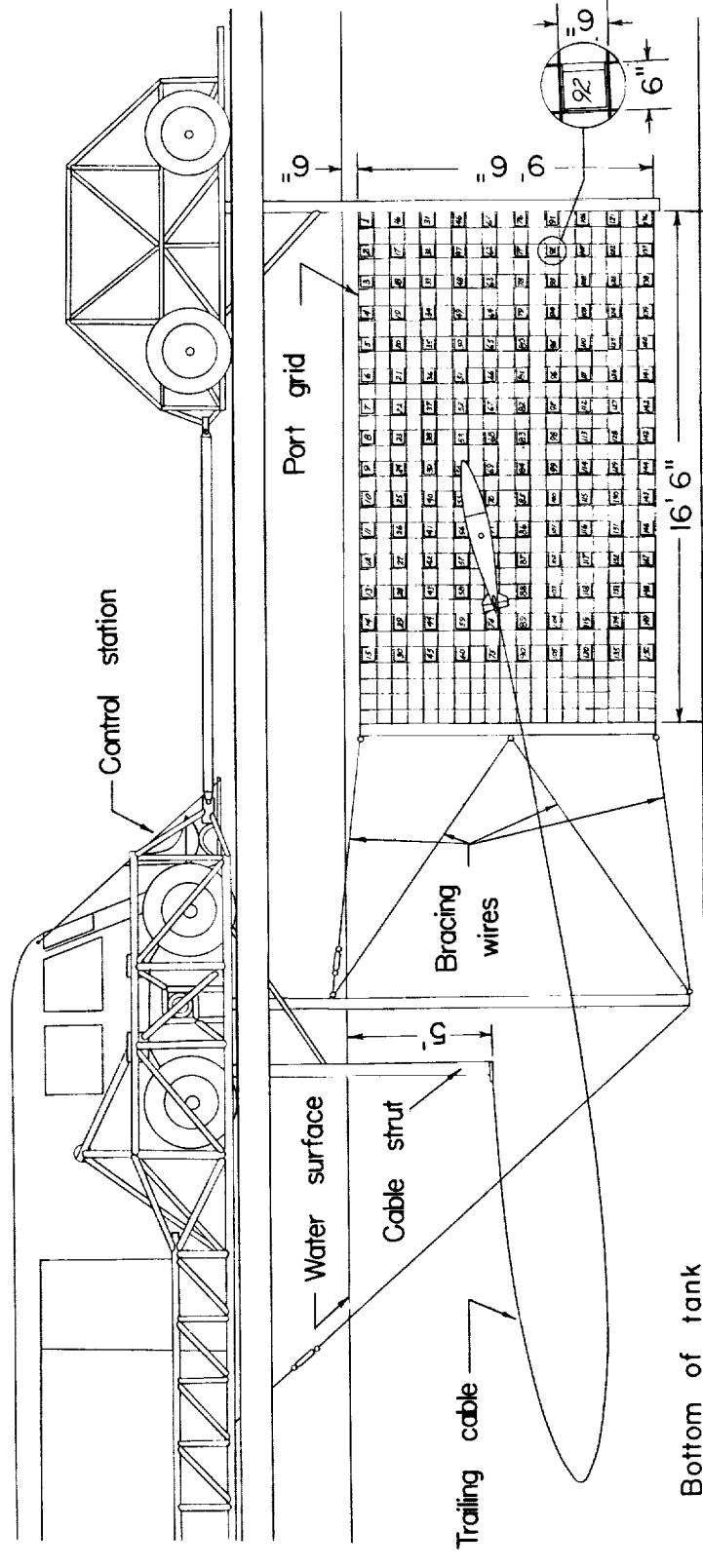
(b) Side view.

Figure 7.- Concluded.
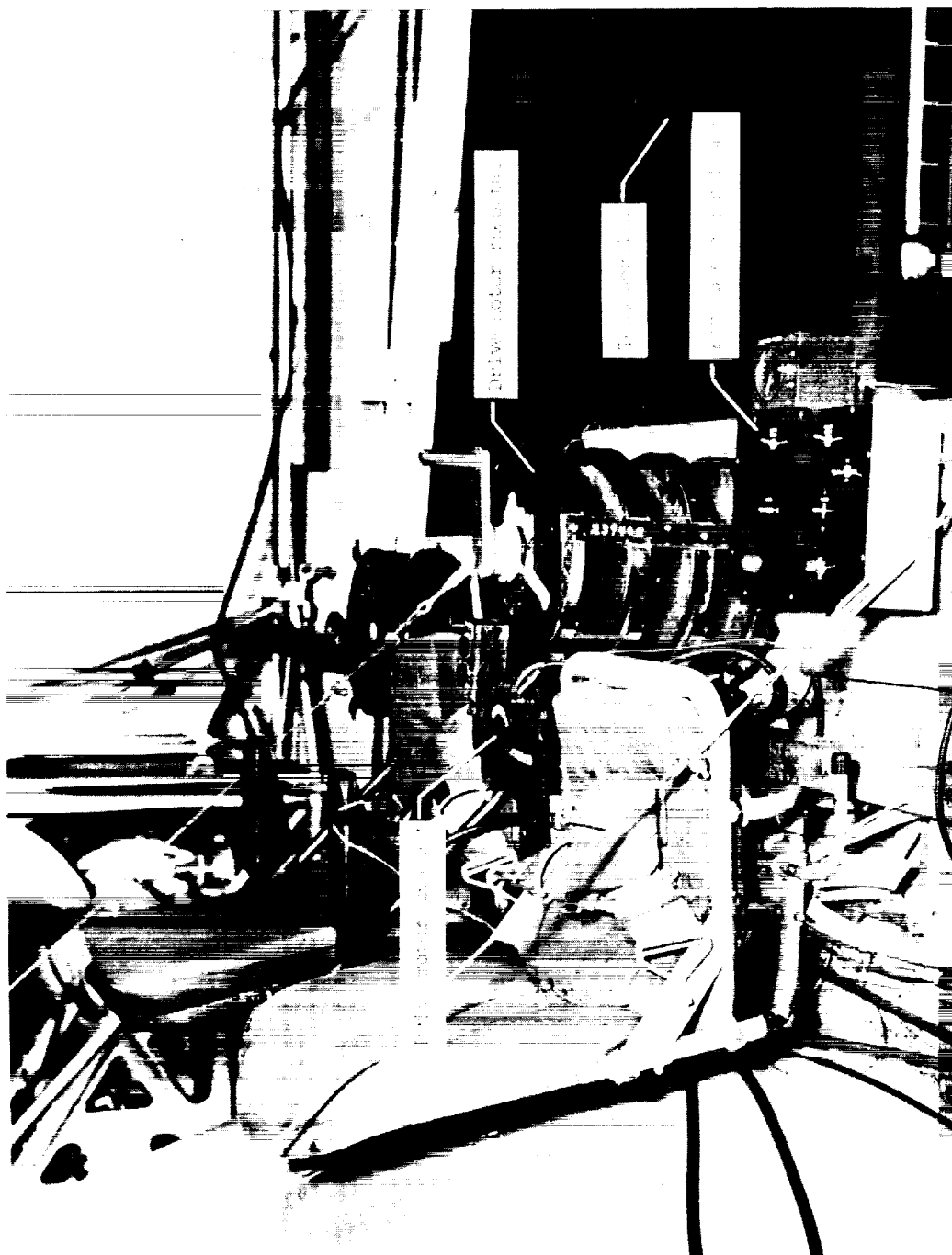
L-83658

Figure 8.- Control station.
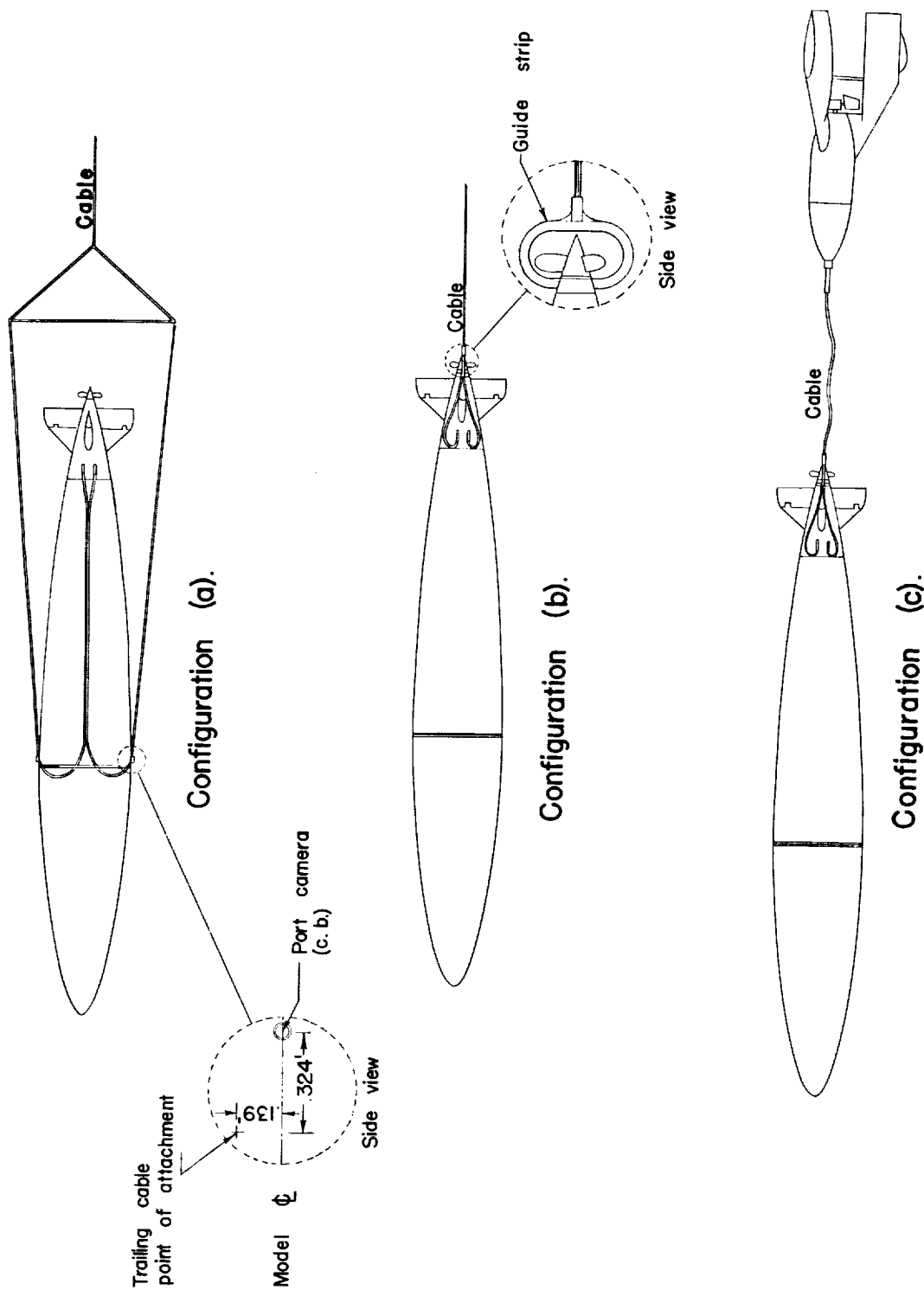
Figure 9.- Cable configurations of Langley tank model 281.
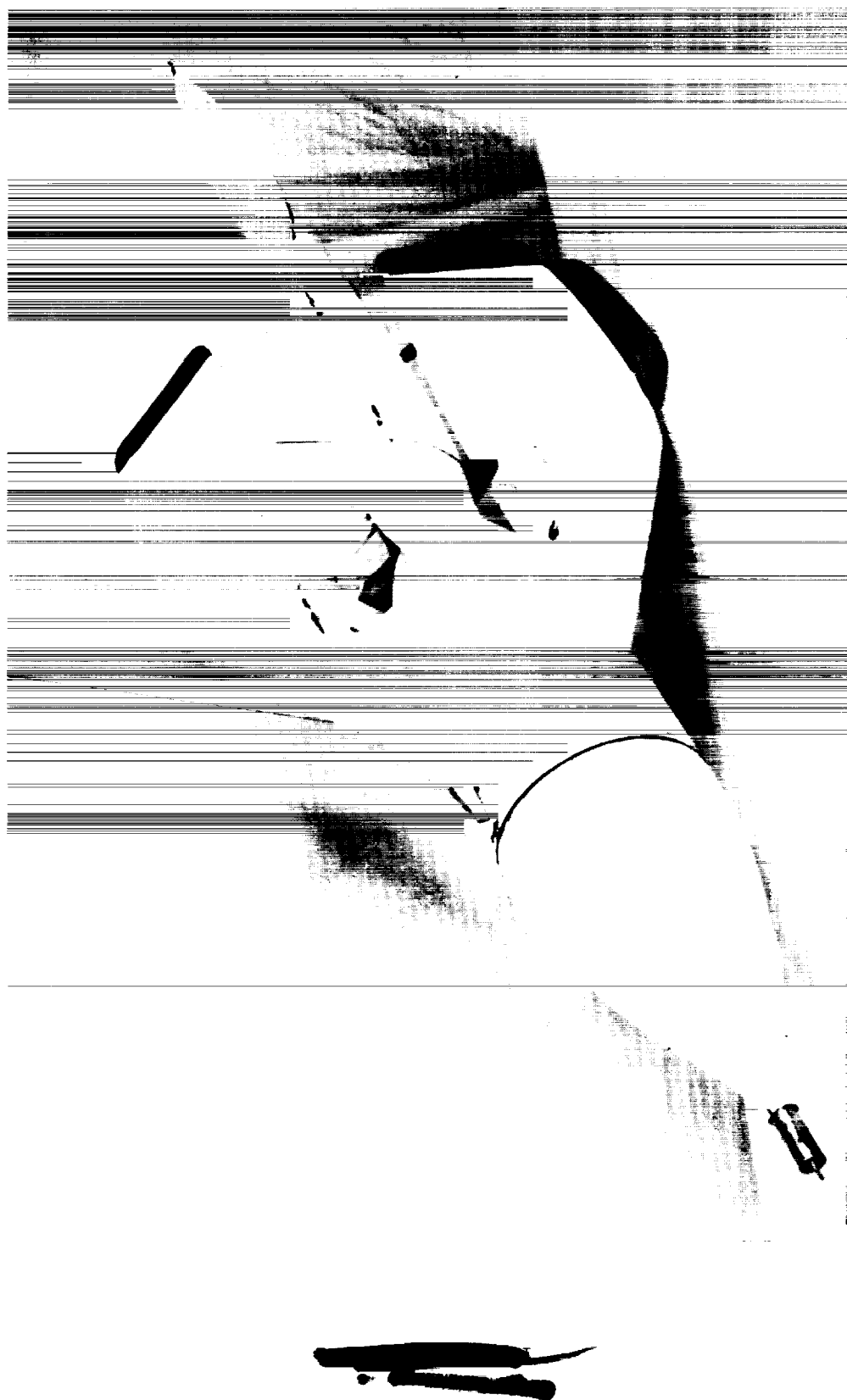
L-83659

Figure 10.- Three-quarter front view of follower for Langley tank model 281.
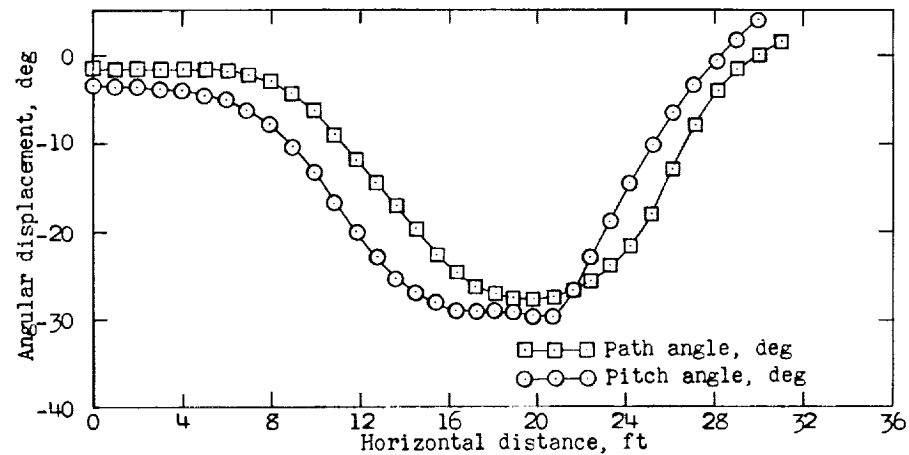
Angular displacement.
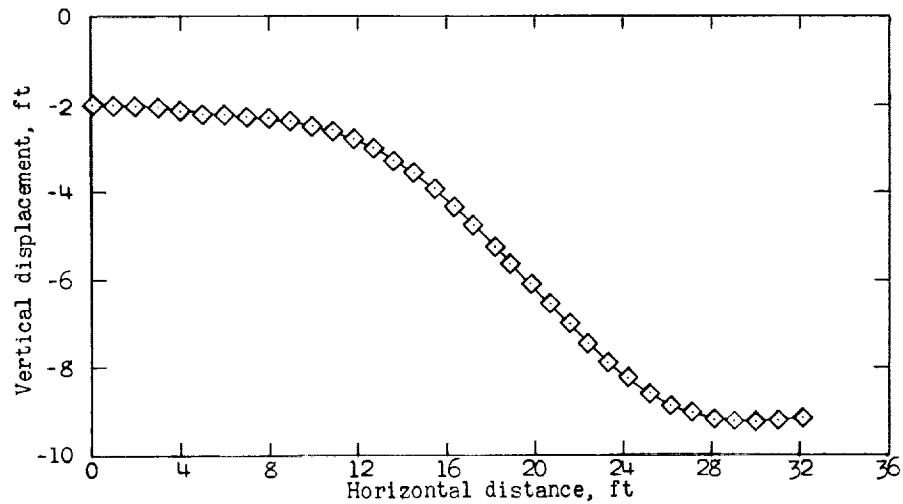
Vertical displacement.
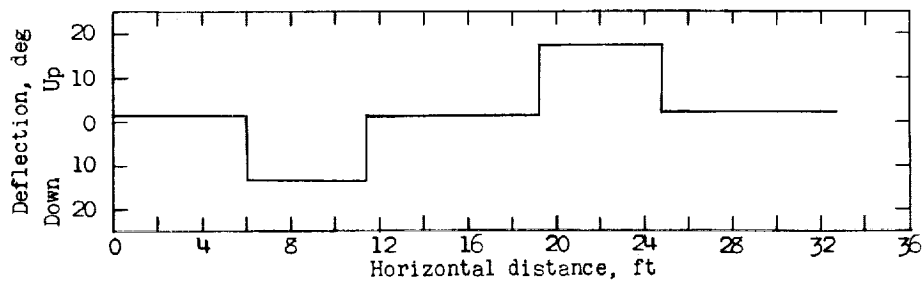
Elevator displacement.

(a) Run 1.

Figure 11.- Motions of model computed from camera records with cable attached near center of buoyancy.
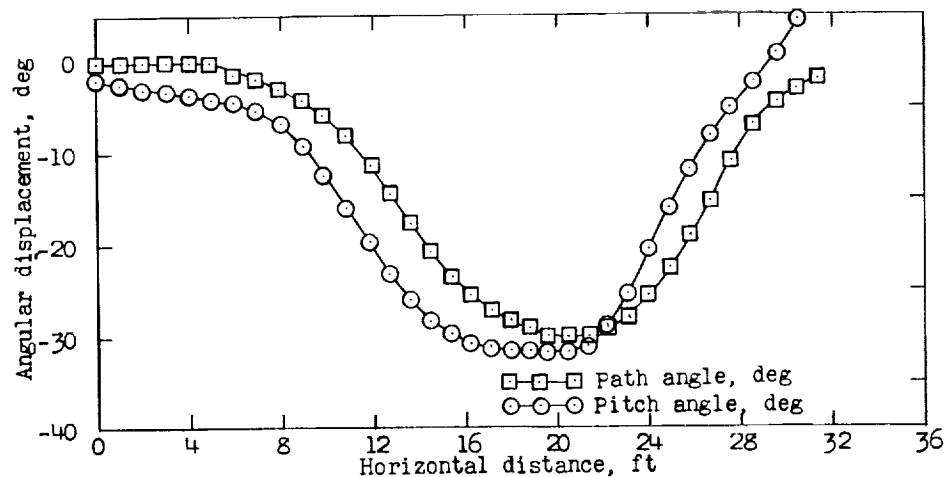
Angular displacement.
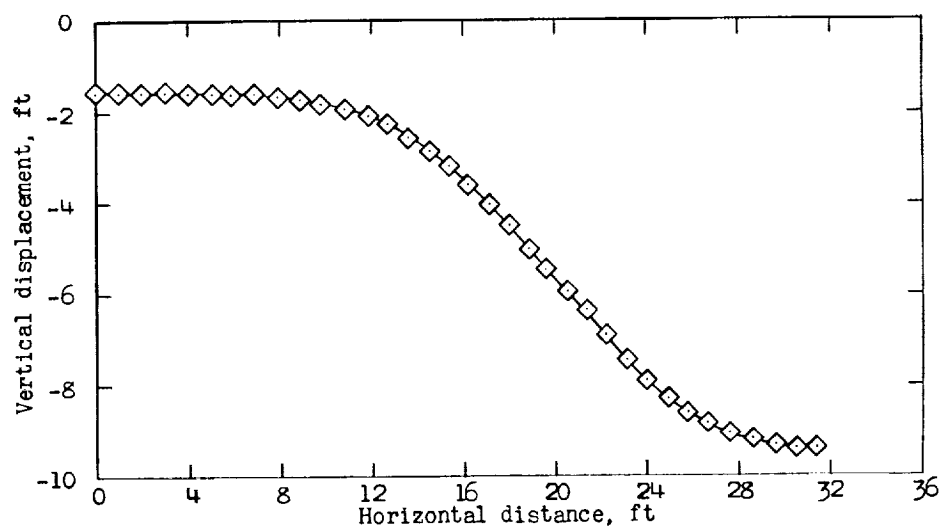
Vertical displacement.
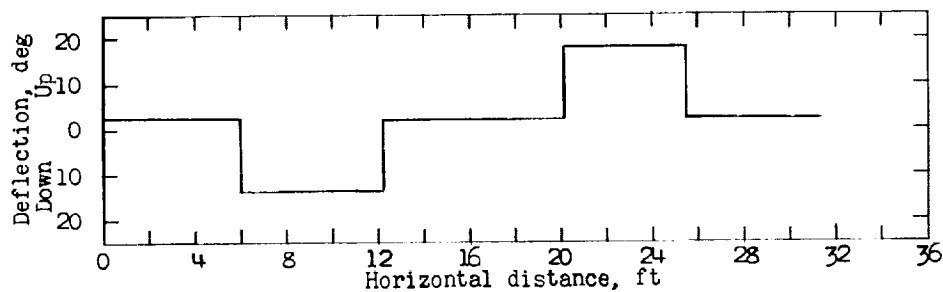
Elevator displacement.

(b) Run 2.

Figure 11.- Concluded.
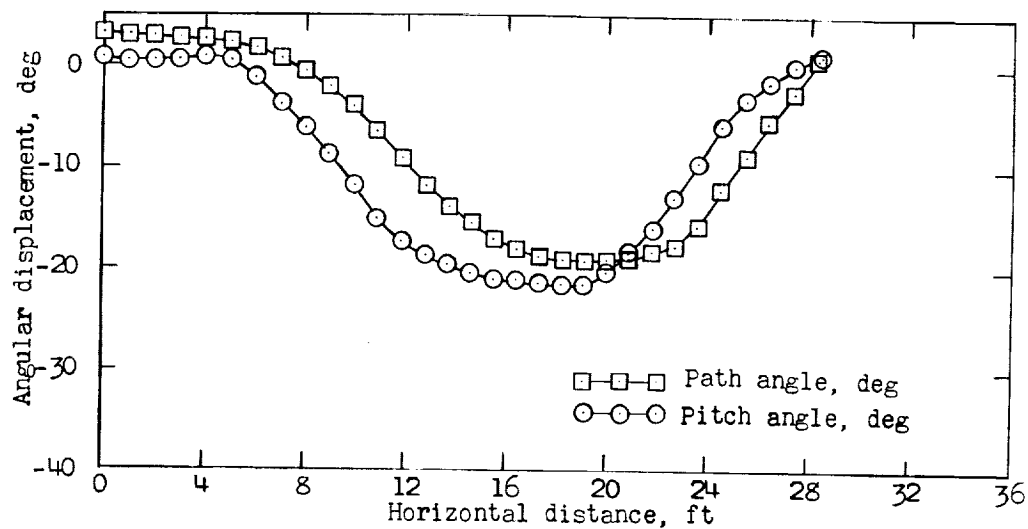
(a) Angular displacement.
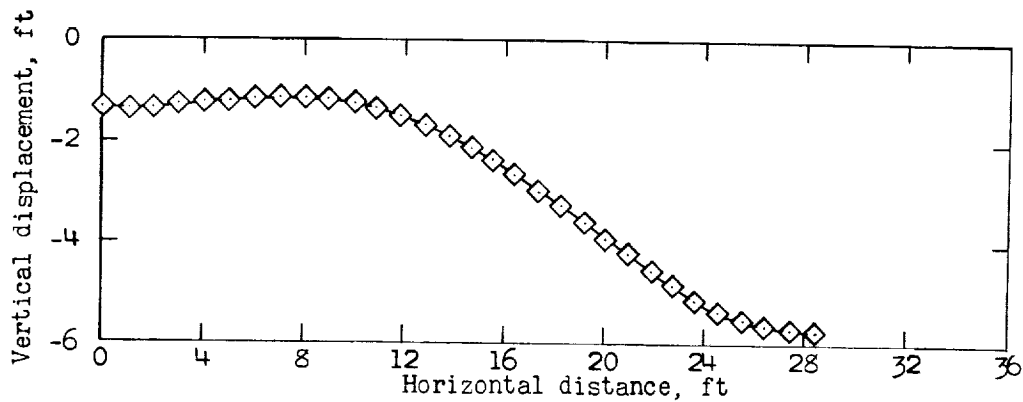
(b) Vertical displacement.
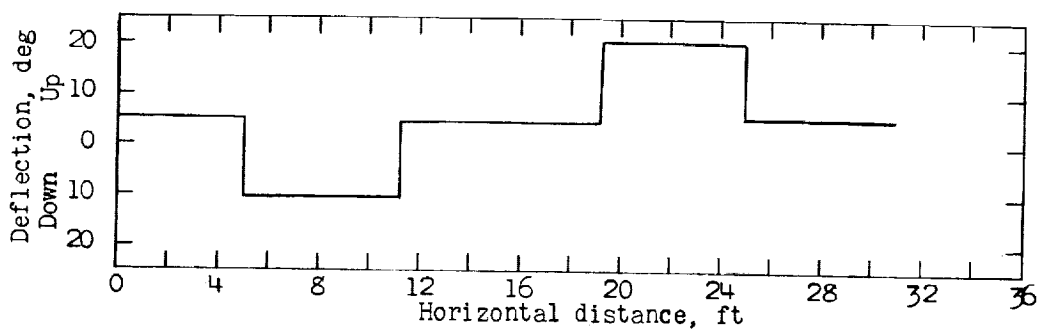
(c) Elevator displacement.

Figure 12.- Motions of model computed from camera records with cable attached at stern. Run 3.
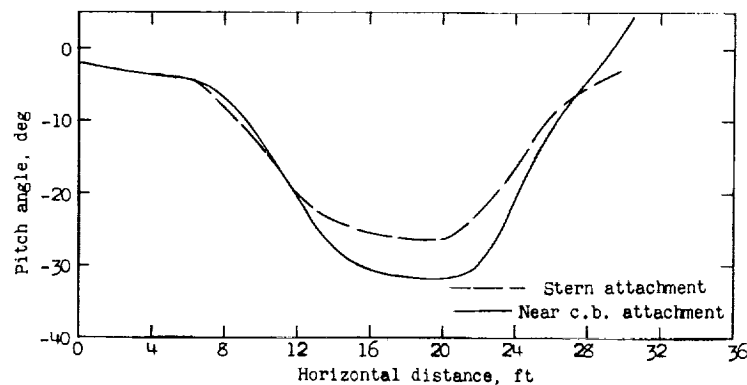
(a) Pitch displacement.
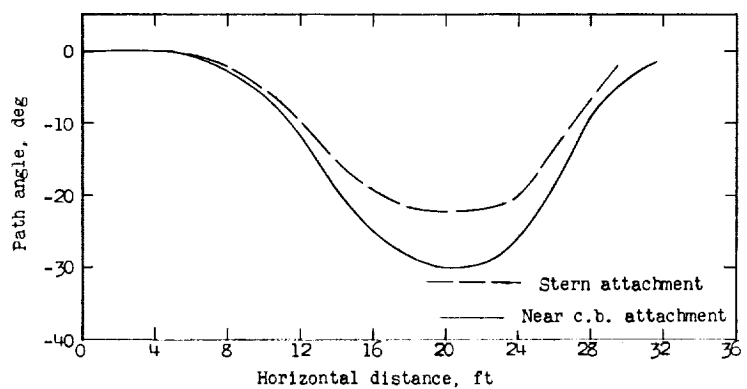
(b) Path displacement.
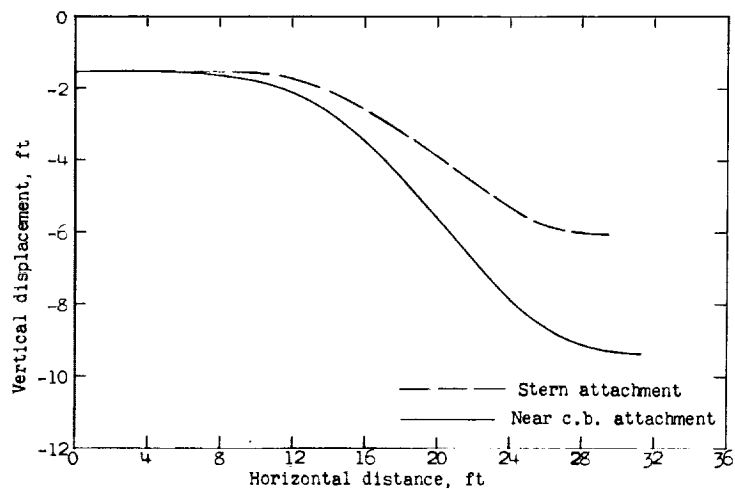
(c) Vertical displacement.

Figure 13.- Comparison of model motions with cable attached at stern and near center of buoyancy.

Figure 14.- Location of weight and cable forces with cable attached near center of buoyancy for two-dimensional case.
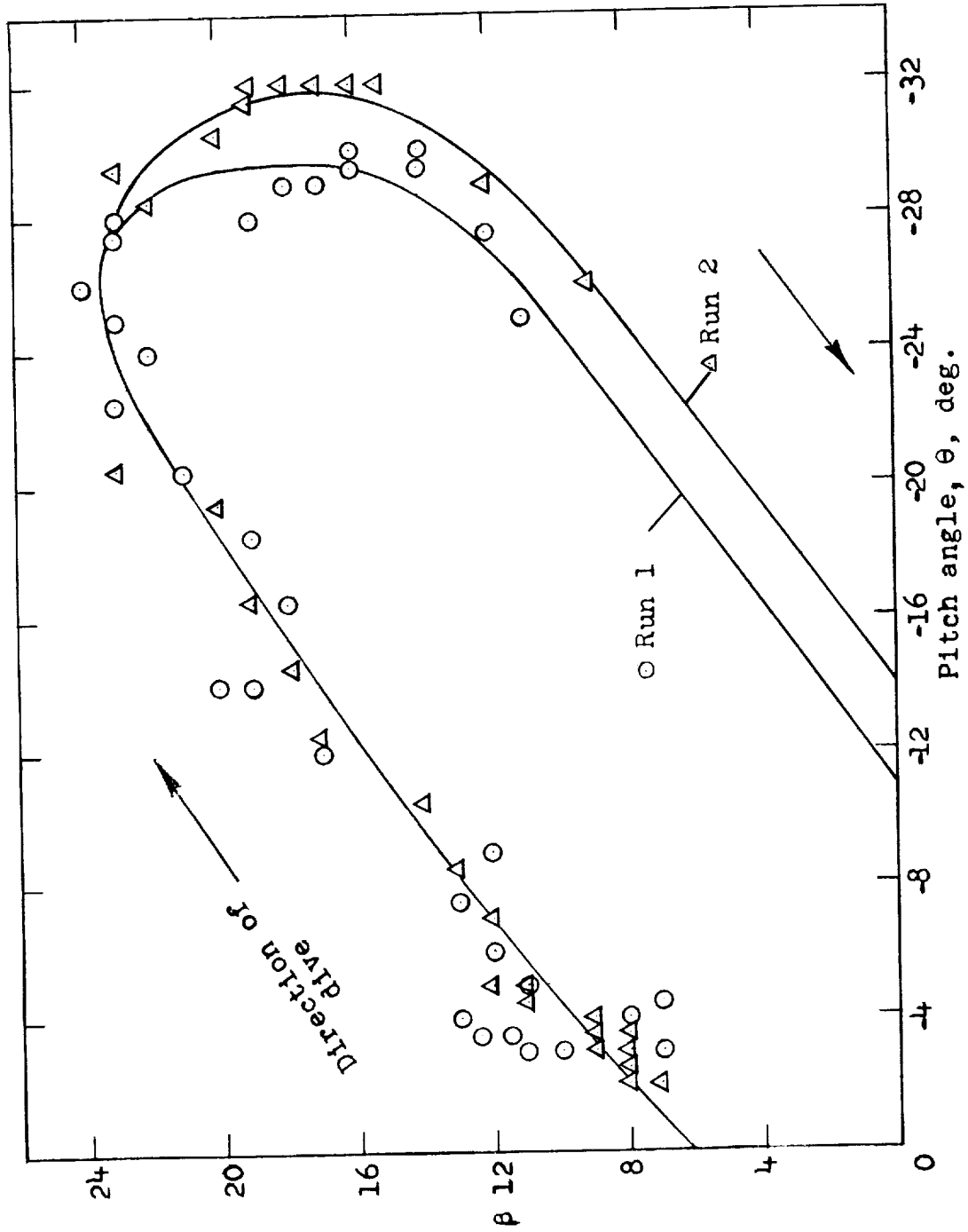
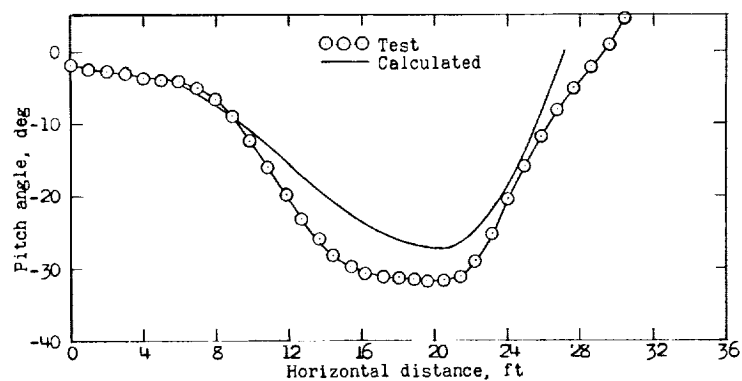Figure 15.- Position of cable during dive maneuver.
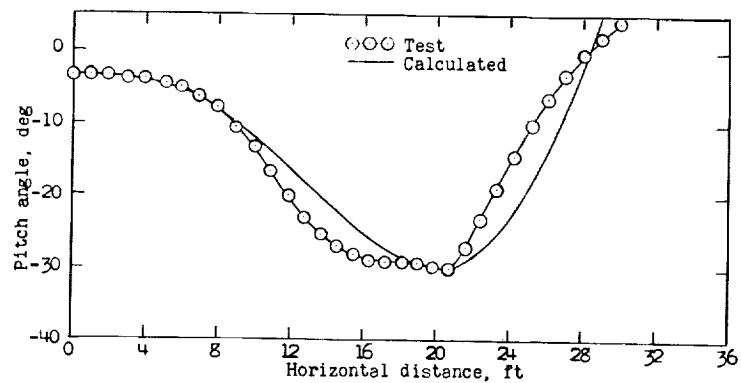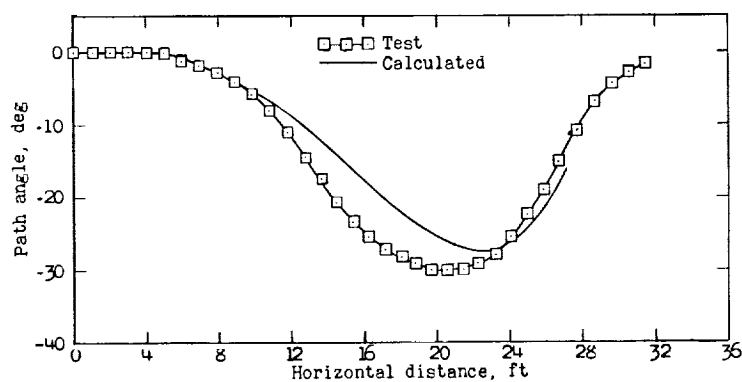
(a) Pitch displacement.
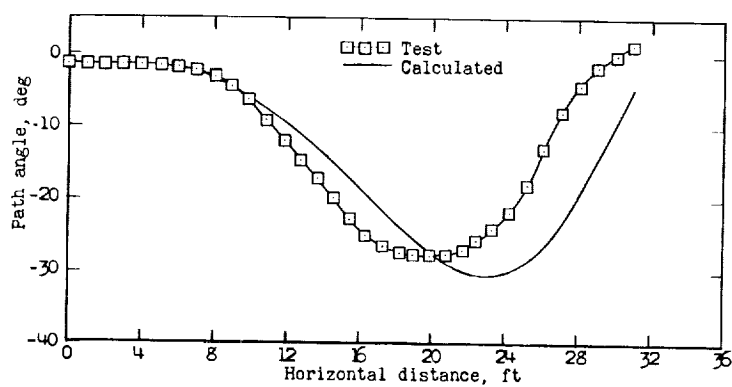
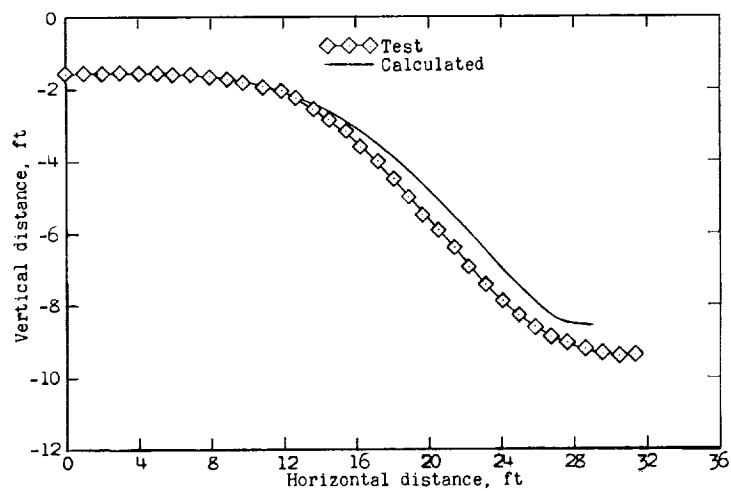(b) Path displacement.
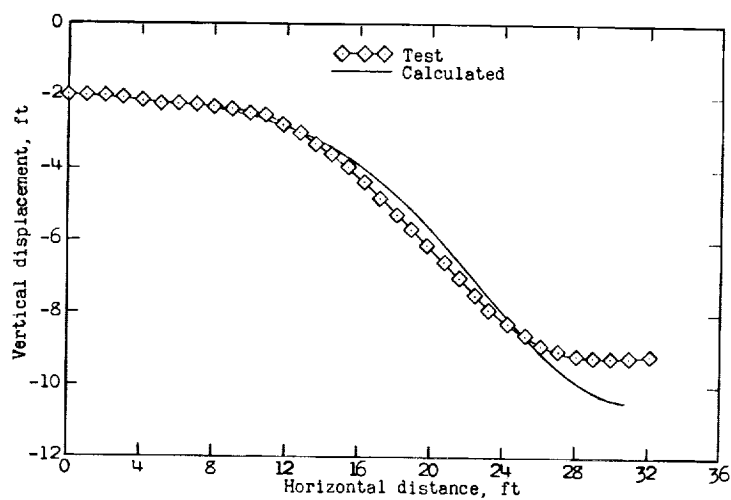
(c) Vertical displacement.

Figure 16.- Comparison of calculated and experimental motions with the cable attached near center of buoyancy. Run 1.

(a) Pitch displacement.

(b) Path displacement.

(c) Vertical displacement.

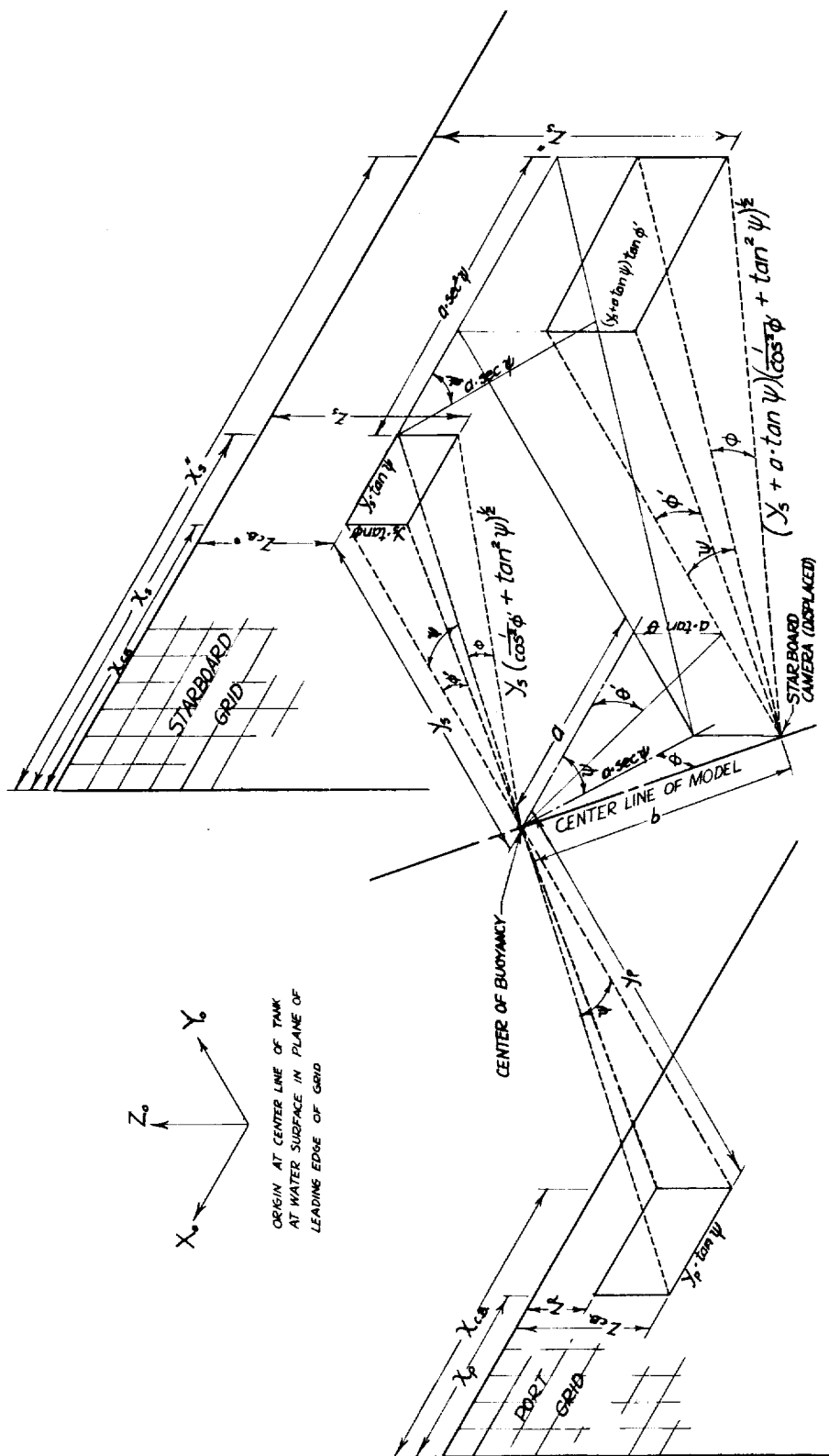Figure 17.- Comparison of calculated and experimental motions with the cable attached near center of buoyancy. Run 2.

Figure 18.- Camera projections on grids.